conclusions. To further investigate the robustness of our results, we presumed that the next three comets observed (thereby increasing the sample size by 60%) have the same rotational properties as Chiron. The one-tailed confidence level for the differences between the near-Earth and comet samples drops from >99% to 95%. For our conclusion that the NEA population is comprised by no more than 40% comet nuclei, the confidence level also drops from 99% to 95%. The robustness arises because the mean values for the current comet sample are so disparate from the asteroid samples that a comparable addition in the opposite tail is needed to offset the difference. Because new values are likely to be centered on the true mean, which is unlikely to be in the opposite tail, it will take a large increase in the sample size to significantly alter the sample mean.

18. R. P. Binzel, thesis, University of Texas, Austin (1986).
19. P. R. Weissman, M. F. A'Hearn, L. A. McFadden, H. Rickman, in *Asteroids II*, R. P. Binzel, T. Gehrels, M. S. Matthews, Eds. (Univ. of Arizona Press, Tucson, 1979), pp. 880–920.

20. Data reported in this paper were obtained in part at the Michigan Dartmouth MIT Observatory. This research was supported by National Science Foundation grant 88-18855 AST (R.P.B.), NASA grant NAGW-1470 (E.B.), and the Lowell Observatory endowment.

3 March 1992; accepted 25 June 1992

Uranium Bioaccumulation by a *Citrobacter* sp. as a Result of Enzymically Mediated Growth of Polycrystalline HUO_2PO_4

Lynne E. Macaskie,* Ruth M. Empson, Anthony K. Cheetham,† Clare P. Grey,‡ A. Jerome Skarnulis§

A *Citrobacter* sp. accumulates heavy deposits of metal phosphate, derived from an enzymically liberated phosphate ligand. The cells are not subject to saturation constraints and can accumulate several times their own weight of precipitated metal. This high capacity is attributable to biomineralization; uranyl phosphate accumulates as polycrystalline HUO_2PO_4 at the cell surface. The precipitated metal is indistinguishable from crystalline $HUO_2PO_4 \cdot 4H_2O$ grown by chemical methods.

A *Citrobacter* sp. accumulates heavy metals as a result of precipitation with enzymically liberated inorganic phosphate (*1*, *2*). This reaction has been harnessed to a biotechnological process for the treatment of metal-bearing streams (*3*, *4*); it also has potential for nuclear waste decontamination (*5*), facilitated by the high radioactive tolerance of the cell-bound phosphate-releasing enzyme (phosphatase) (*6*). The immobilized whole-cell biocatalyst tolerates loads of up to 9 g of accumulated uranium per gram of biomass (900% of the cellular dry weight) over several weeks without apparent ill effect (*4*). A packaging mechanism for the U might be postulated to permit enzyme turnover, yet the high toxicity of uranyl ion (*7*) makes a biochemical compartmentalization on this scale unlikely. With a continuous supply of organic phosphate donor molecules to cells immobilized in a flow-through cartridge ("bioreactor"), a steady state is rapidly achieved whereby metal is removed continuously and efficiently from the flow with a corresponding accumulation of metal within the bioreactor (*3*).

In this study we used electron microscopy to examine the mechanisms of metal accumulation and the fate of individual cells subjected to uranyl ion loading. The cells were not fixed or stained in any way, and, as such, before U challenge they were indistinct, and there was no accumulation of electron-dense material (Fig. 1A). Cells challenged in suspension with uranyl nitrate and phosphatase substrate for 12 hours accumulated U to about 250% of the bacterial dry weight (*8*) and were highly electron-opaque with little visible surface detail (Fig. 1B). Dried, ground samples of the loaded cells were lemon yellow in color and exhibited fluorescence characteristic of uranyl compounds. A video image of a cell revealed areas of enhanced electron opacity, primarily at the cell periphery (Fig. 1C), which we analyzed further by imaging for U (Fig. 1D) and phosphorus (Fig. 1E), using the x-ray emissions characteristic of these elements (U $L\alpha$ and P K).

Clear evidence for codeposition suggests that a form of uranium phosphate had been produced. X-ray microanalysis of specimen microareas (Fig. 1F) indicates that cells unchallenged with the uranyl ion showed x-ray emissions attributable to the low level of P associated with biological material, as well as the copper present in the grid. Qualitatively, the cellular deposit is indistinguishable from a hydrogen uranyl phosphate standard ($HUP{:}HUO_2PO_4 \cdot 4H_2O$) (Fig. 1F). Quantitative comparisons were made by integration of the areas under the U $L\alpha$ and P K peaks and were interpreted by the ratio method (*9*): $X_1/X_2 = kI_1/I_2$, where k is a constant and X_1, X_2, I_1, and I_2 represent, respectively, the concentrations and the emission intensities of the two elements. These data do not provide information on the absolute amounts of U and P accumulated, but the peak ratio can be used for comparison with the corresponding ratio obtained using the known atomic ratio of U to P in the HUP standard (U:P ratio = 1:1). The ratio of the peak areas for the standard was 1.91 ± 0.048, while that for the accumulated material was 1.75 ± 0.15 (mean ± standard errors from 15 and 10 determinations, respectively). These values are not significantly different at $P = 0.95$; taking into account that the cell also contains "biological" P (which would tend to reduce the peak area ratio), we conclude that the atomic U:P ratio in the cellular deposit is close to 1:1. However, this ratio could also be given by other uranium phosphates, and, as confirmation that HUP has indeed been formed, we examined the standard and accumulated material by solid-state infrared spectroscopy, x-ray diffraction, and magic angle spinning nuclear magnetic resonance (MASNMR).

The HUP standard was prepared by the method of Weigel and Hoffman (*10*), and its x-ray diffraction pattern was found to be in good agreement with the published data for HUP (*10*, *11*). Infrared spectroscopy was performed in a carrier of cesium chloride at a weight:weight ratio of ground standard or ground U–loaded biomass to CsCl of 1:30. The spectra were very similar, with strong absorption peaks at 930 nm characteristic of the uranyl ion (*12*). We conclude that the accumulated material is a form of uranyl phosphate.

Further analyses with ^{31}P MASNMR indicated that proton-decoupled spectra from the U-loaded cells and the uranyl phosphate standard exhibit resonances at similar isotropic chemical shifts (σ_{iso} = 22.7 and 19.5 ppm, respectively) and have similar side-band intensities. Both the isotropic shift and the chemical shift anisotropy can be used to identify the phosphate species present. In general, pyrophosphates resonate upfield from the corresponding orthophosphate compounds (*13*), and hence the similar isotropic chemical shift for the uranyl phosphate standard and loaded cells confirmed that phosphate groups

L. E. Macaskie, School of Biological Sciences, University of Birmingham, Edgbaston, Birmingham, B15 2TT, United Kingdom.
R. M. Empson, Saint Mary's Hospital Medical School, Praed Street, London, W21NY, United Kingdom.
A. K. Cheetham, C. P. Grey, A. J. Skarnulis, Laboratory of Chemical Crystallography, University of Oxford, Parks Road, Oxford, OX1 3PD, United Kingdom.

*To whom correspondence should be addressed.
†Present address: Materials Department, University of California, Santa Barbara, CA 93106.
‡Present address: Molecular Spectroscopy Laboratory, Faculty of Physical Sciences, Tooerniveld, University of Nijmegen, Nijmegen, The Netherlands 6525 ED.
§Present address: Jeol Systems U.K. Ltd., Jeol House, Silver Court, Watchmead, Welwyn Garden City, Herts, AL7 1LT, United Kingdom.

were present in both materials. Spinning side-band analysis (*14*) of spectra collected at spinning speeds of 1500 Hz gave values for the chemical shift tensors σ_{11}, σ_{22}, and σ_{33} (*14*) of 32.5 ± 2, 20 ± 4, and 6 ± 3 ppm for $HUO_2PO_4 \cdot 4H_2O$ and 35 ± 2, 28 ± 4, and 5 ± 2 as the major resonances from the loaded cells. These are in the range expected for phosphate, PO_4^{3-}, units as opposed to HPO_4^{2-} units (*15*) and more condensed phosphate species (for example, P_2O_7) (*16*, *17*).

The structure of HUP may be described as comprising layers of UO_2PO_4 between which the H^+ ions are held in a two-dimensional network of water molecules (*18*). The H^+ ions are highly mobile within the water layers (*19*). We suggest that the nascent PO_4^{3-} from the enzymic reaction self-assembles with UO_2^{2+} to form a crystal that is extruded from the loci of phosphatase activity and that water hydrogen bonding assists in the formation of an ordered structure (*18*).

Electron diffraction patterns of the cell-bound material (Fig. 2) are suggestive of a two-dimensional fibrous structure, which is consistent with the known structure of HUP. Evidence for the deposition of fibrillar structures was sought. Examination of a lightly loaded cell revealed faint "brush-like" extrusions from the cell surface (Fig. 3A). These appeared as electron-dense fibrils less than 100 Å in diameter; this is of the correct width according to the published structure for HUP (*18*), but precise measurements were not performed. More heavily loaded cells tended to disintegrate in the electron beam under high vacuum, leaving particles of deposited material as a cell ghost (*2*) (Fig. 3B). Here needles of

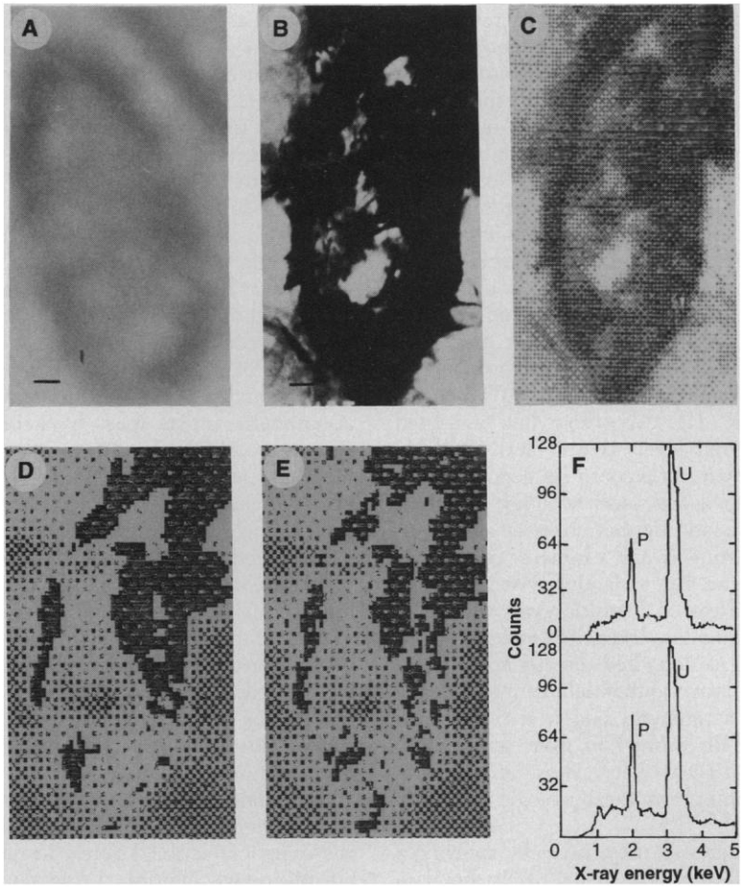

Fig. 1. Accumulation of uranium by *Citrobacter* sp. and characterization of the accumulated metal precipitate (*20*). Uranium-unsupplemented cells (**A**) are indistinct, whereas in U-challenged cells the U is visible as an electron-opaque stain, obscuring cellular detail (**B**). A computer video image (**C**) reveals deposition patterns not visible in the native specimen, and further imaging for U (**D**) and P (**E**) shows codeposition of the two elements. The data were obtained with the Jeol instrument in conjunction with an energy-dispersive x-ray spectrometer (Tracor), which allows elementary analysis of specimen microareas (*2*). In the quantitative analysis of specimen microareas (<1 μm^2) we used the x-ray emissions characteristic of U and P to allow calculation of relative peak areas for U and P for the U-loaded cells (**F, bottom**) and compared them to a hydrogen uranyl phosphate standard (HUP: $HUO_2PO_4 \cdot 4H_2O$) (**F, top**) prepared according to published methods (*11*), and with its identity confirmed by x-ray powder diffraction analysis referenced to published standards (*11*, *12*). X-ray spectra were accumulated for 100 s, and data analyses were done with a Tracor TN-5500 system. Total data accumulation was 128 by 128 pixels; total run time was several hours. Scale bars represent 100 nm.

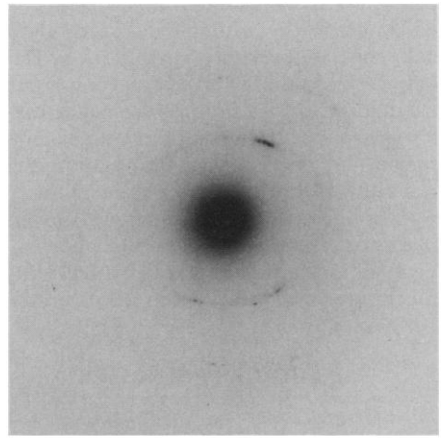

Fig. 2. Electron diffraction pattern of the accumulated material, acquired using the Jeol electron microscope (see legend to Fig. 1).

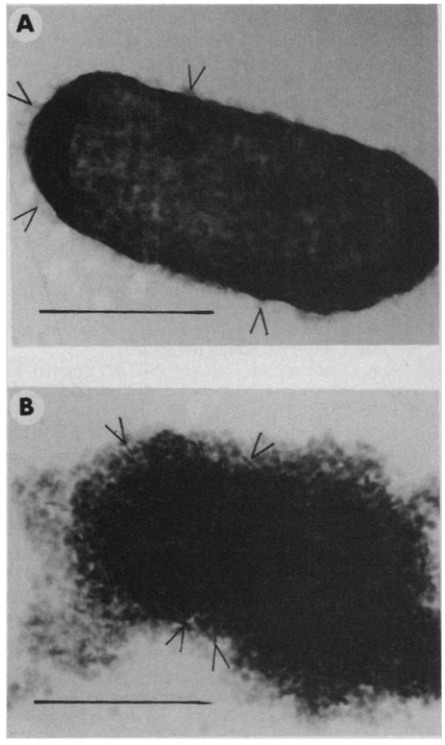

Fig. 3. Detail of the accumulated uranyl phosphate. Under heavy metal loading the cells often lost integrity in the electron beam under high vacuum (*2*), but the accumulated material is evident as granular or needle-like deposits (**B**; arrows). A lightly loaded cell retained integrity, with exocellular electron-dense material visible as brush-like extrusions (**A**; arrows). Individual fibrils are estimated to be less than 100 Å thick (bar = 1 μm). Clumped extrusions are also apparent.

precipitate were visible, interspersed within a more particulate matrix. Possibly the particles represent aggregates of precipitate; the brush-like extrusions in the lightly loaded cell (Fig. 3A) apparently occur in discrete clumps, presumably corresponding to loci of phosphatase activity.

Whether the example of biocatalytically mediated crystal growth used by this *Citrobacter* sp. has evolved as a generalized mechanism of defense against metal toxicity by exocellular compartmentalization remains to be confirmed. Similarly, it is not known what role, if any, the architecture or integrity of the outer wall layers plays, or, indeed, whether the phosphatase itself is located in juxtaposition to the precipitate or distanced from it, within the periplasmic space.

REFERENCES AND NOTES

1. R. M. Aickin, A. C. R. Dean, A. K. Cheetham, A. J. Skarnulis, *Microbios Lett.* **9**, 7 (1979).
2. L. E. Macaskie, A. C. R. Dean, A. K. Cheetham, R. J. B. Jakeman, A. J. Skarnulis, *J. Gen. Microbiol.* **133**, 539 (1987).
3. L. E. Macaskie and A. C. R. Dean, *Adv. Biotechnol. Processes* **12**, 159 (1989).
4. L. E. Macaskie, *J. Chem. Technol. Biotechnol.* **49**, 357 (1990).
5. _____, *Crit. Rev. Biotechnol.* 11, 41 (1991).
6. L. Strachan, L. E. Macaskie, B. C. Jeong, in *Proceedings of the 201st American Chemical Society Meeting* (American Chemical Society, Washington, DC, 1991), vol. 31, p. 128.
7. E. J. Plummer and L. E. Macaskie, *Bull. Environ. Contam. Toxicol.* **44**, 173 (1990).
8. L. E. Macaskie, J. D. Blackmore, R. M. Empson, *FEMS Microbiol. Lett.* **55**, 157 (1988).
9. G. Cliff and G. W. Lorimer, *J. Microsc. (Oxford)* **103**, 203 (1975).
10. F. Weigel and G. Hoffman, *J. Less Common Met.* **44**, 99 (1976).
11. H. W. Dunn, *Oak Ridge Natl. Lab. Publ. 2092* (1956).
12. C. Greaves, A. K. Cheetham, B. E. F. Fender, *Inorg. Chem.* **12**, 3003 (1973).
13. A. K. Cheetham, N. J. Clayden, C. M. Dobson, R. J. B. Jakeman, *J. Chem. Soc. Chem. Commun.* **1986**, 195 (1986).
14. J. Herzfeld and A. C. Berger, *J. Chem. Phys.* **73**, 6021 (1980).
15. W. O. Rothwell, J. S. Waugh, J. P. Yesinowski, *J. Am. Chem. Soc.* **102**, 2637 (1980).
16. A. R. Grimmer and U. Haubenreisser, *Chem. Phys. Lett.* **99**, 487 (1983).
17. T. M. Duncan and D. C. Douglass, *Chem. Phys.* **87**, 339 (1984).
18. B. Morosin, *Acta Crystallogr. Sect. B* **34**, 3732 (1978).
19. A. T. Howe and M. G. Shilton, *J. Solid State Chem.* **34**, 149 (1980).
20. *Citrobacter* sp. was pregrown to the midlogarithmic phase in minimal medium containing glycerol and glycerol 2-phosphate as the respective C and P sources (*8*). Cell harvests were resuspended in 2 mM citrate buffer (pH 6.9) supplemented with glycerol 2-phosphate (to 5 mM) and uranyl nitrate (to 1 mM) for 12 hours, to a final loading of U of about 250% of the cellular dry weight (*8*). In the examination of samples we used a Jeol JEM-2000 FX electron microscope with an accelerating voltage of 200 keV (*1, 2*).

21. Financial support was provided by BTP Ltd., in association with Pembroke College, University of Oxford (to L.E.M.) and by the Science and Engineering Research Council (to A.K.C. and C.P.G.).

10 March 1992; accepted 29 May 1992

Increasing Rates of Atmospheric Mercury Deposition in Midcontinental North America

Edward B. Swain,* Daniel R. Engstrom, Mark E. Brigham,† Thomas A. Henning,‡ Patrick L. Brezonik

Mercury contamination of remote lakes has been attributed to increasing deposition of atmospheric mercury, yet historic deposition rates and inputs from terrestrial sources are essentially unknown. Sediments of seven headwater lakes in Minnesota and Wisconsin were used to reconstruct regional modern and preindustrial deposition rates of mercury. Whole-basin mercury fluxes, determined from lake-wide arrays of dated cores, indicate that the annual deposition of atmospheric mercury has increased from 3.7 to 12.5 micrograms per square meter since 1850 and that 25 percent of atmospheric mercury deposition to the terrestrial catchment is exported to the lake. The deposition increase is similar among sites, implying regional or global sources for the mercury entering these lakes.

Mercury (Hg) contamination has been documented in many lakes in remote regions of Canada, Sweden, Finland, and the United States, including Minnesota, Wisconsin, and Florida. Although these lakes lie in landscapes with little or no human development, they contain fish with Hg levels that pose health risks for human consumption (*1, 2*), and their sediments show stratigraphic evidence of increasing Hg inputs within the last 100 to 200 years (*3, 4*). Most researchers have concluded that the Hg contamination must derive from atmospheric pollution.

Despite considerable research on Hg in the environment, the extent to which atmospheric Hg deposition has increased from natural levels is not clear. Reliable measurements of modern Hg deposition are limited to a few years at a few locations (*5–7*), historic deposition rates are essentially unknown, and estimates of the anthropogenic Hg emissions that might be driving increased deposition vary widely (*2, 8–11*). In remote lakes, it is uncertain how much Hg is deposited directly to the lake surface relative to that delivered to the lake from its catchment, and it is not known whether Hg washed in from surrounding soils is derived solely from atmospheric deposition or from local geologic sources as well.

We addressed these issues by applying a simple mass-balance model to Hg flux data generated from the sediments of seven relatively undisturbed lakes in Minnesota and Wisconsin. Whole-basin Hg accumulation rates are calculated for each lake from multiple (7 to 15) sediment cores that were analyzed stratigraphically for Hg and dated by ^{210}Pb (*12*). By comparing whole-basin Hg fluxes from a group of lakes in a geographic region, we are able to estimate atmospheric deposition rates for modern and preindustrial times and the contribution of Hg from the catchments surrounding the lakes.

Mercury has been measured in sediment cores from other remote or rural lakes (*13, 14*), but conclusions are limited to a description of Hg accumulation at a single core site and the qualitative statement that atmospheric inputs must have increased. Because sediment deposition patterns and metal concentrations are spatially variable across a lake basin, Hg accumulation rates from a single core cannot be automatically extrapolated to the entire lake (*15*). Whole-basin studies of heavy-metal accumulation (*16, 17*), including one for Hg (*3*), have been done before but are rare because of the large effort required to analyze and date multiple cores representing the various depositional environments in a single basin. None of these studies used dated cores to calculate explicitly whole-basin metal fluxes for more than one lake.

The study sites include four lakes from the Superior National Forest in northeastern Minnesota (Thrush, Dunnigan, Meander, and Kjostad), Cedar Lake in central Minnesota, Mountain Lake in southwestern Minnesota, and Little Rock Lake in northern Wisconsin (Fig. 1). All of the lakes lie in mixed deciduous-conifer forest, except for Mountain Lake, which is in native tall-grass prairie. Precipitation and wet sulfate deposition increase from west to east across the region (*18*). The lakes are uniformly small and shallow and are fed principally by ground-water seepage and surface precipitation (Table 1). Water residence times are short, except for the two

E. B. Swain, Minnesota Pollution Control Agency, 520 Lafayette Road, St. Paul, MN 55155.
D. R. Engstrom, Limnological Research Center, University of Minnesota, Minneapolis, MN 55455.
M. E. Brigham, T. A. Henning, P. L. Brezonik, Department of Civil and Mineral Engineering, University of Minnesota, Minneapolis, MN 55455.

*To whom correspondence should be addressed.
†Present address: U.S. Geological Survey, District Office, St. Paul, MN 55101.
‡Present address: James M. Montgomery Consulting Engineers, Wayzata, MN 55391.